ELSEVIER

Journal of Applied Geophysics 34 (1996) 187–198

APPLIED GEOPHYSICS

DC resistivity and IP methods in acid mine drainage problems: results from the Copper Cliff mine tailings impoundments

Yuval, Douglas W. Oldenburg

U.B.C.-Geophysical Inversion Facility, Department of Geophysics and Astronomy, University of British Columbia, Vancouver, B.C. V6T 1Z4, Canada

Received 4 May 1995; accepted 8 September 1995

Abstract

Oxidation of sulfide minerals in the mine tailings impoundments at Copper Cliff, Ontario generates acidic conditions and elevated concentrations of dissolved metals and sulfates in the pore water. The pore water migrates away from the tailings to pose a potential environmental hazard if it should reach nearby water systems. There is a need to characterize this potential environmental problem and to assess the future hazards. A combined DC resistivity and induced polarization (IP) survey was carried out along one of the major flowpaths in the tailings and the data were inverted to produce detailed electrical conductivity and chargeability structures of the cross-section below the survey line. The conductivity distributions are directly translated, through theoretical and empirical relations, to a map of the concentration of the total dissolved solids (TDS) along the cross-section and thereby provide insight about the in-situ pore water quality. The sulfide minerals are the source of the IP response and, thus, when combined with borehole data, the chargeability model can be used to estimate the amount and distribution of the sulfides.

1. Introduction

When sulfide minerals are exposed to water and oxygen they oxidize to form soluble metals and sulfates. Products of the oxidation contribute to the acidity in the oxidizing site and, in the absence of alkalinity to neutralize the acidity, the pH level can drop significantly. The elevated solubility of metals in acidic water prevents their precipitation and results in high concentrations of dissolved metals and salts in the acidic water. Eventually, surface water will enter the acid generating site to transport the contaminants toward groundwater systems and surficial water bodies.

The DC resistivity method has been used for many years to identify and delineate the boundaries of contaminated water plumes from landfills (Stollar and Roux, 1975; Kelly, 1976; Urish, 1983; Carpenter et al., 1990) and acid generating mines (Merkel, 1972; Ebraheem et al., 1990). Most investigators used horizontal profiling to delineate the lateral extent of the contamination and vertical sounding to get information about its stratigraphy. Interpretation of the profile data has usually been made directly from the apparent conductivity maps while the sounding data are analyzed using various curve matching techniques. Carpenter et al. (1990) applied a Marquardt inversion procedure, combined with curve matching, to their sounding data but their model is one-dimensional and the number of layers is limited.

Applications of the IP method to contamination problems have recently appeared in the literature. Frangos and Andrezal (1994) and Draskovits (1994) investigated IP responses in waste sites in eastern Europe. Wardlaw and Wagner (1994) carried out an

SSDI 0926-9851(95)00020-8

IP survey over the Fraser Pond on the edge of the Sudbury basin, Ontario and identified zones of high sulfide concentration within the rock pile and in the underlaying tailings. Their suggestion of a linear relationship between the maximum apparent chargeability and sulfide concentration is encouraging in that it shows that IP measurements have the potential for producing estimates of sulfide concentrations. Unfortunately each apparent chargeability datum is an average of the intrinsic chargeability of a volume of rock in the vicinity of the electrodes. Therefore, even if intrinsic chargeability is linearly related to sulfide concentration, then that relationship will be distorted when there is spatial distribution of sulfides. A better approach might be to invert the field data to first recover an estimated distribution of chargeability and then formulate a relationship between intrinsic chargeability and sulfide content.

In this paper we investigate the potential for using DC resistivity and IP data to obtain quantitative information about the amount of total dissolved solids in the tailings water and to estimate sulfide concentration. The DC resistivity and IP data from the Copper Cliff tailings site are inverted to recover a 2-D cross-section of conductivity and chargeability. Simple calculations of conductivity as a function of known TDS concentrations are in a good agreement with the inversion results, implying that the TDS concentration might be directly calculated from the inverted conductivity section. Obtaining estimates of sulfide content from IP data is more problematic and requires borehole constraint information.

2. The study area

The International Nickel Company (INCO Ltd.) operates a large complex of mining, milling, smelting, and refining facilities in the Sudbury district, Northern Ontario (see Fig. 1). Ore extracted from the sublayer of the Sudbury Igneous Complex, containing up to 60 wt% sulfides, is processed to produce nickel, copper, cobalt, and precious metals. Since the 1930s the recovery has been based on the metal-concentration process which results in the production of mill tailings. The tailings have been dumped into nearby impoundments, i.e. regions of surface stockpiling, and currently cover an area of 21 km^2. A map of the impoundments is shown in Fig. 2.

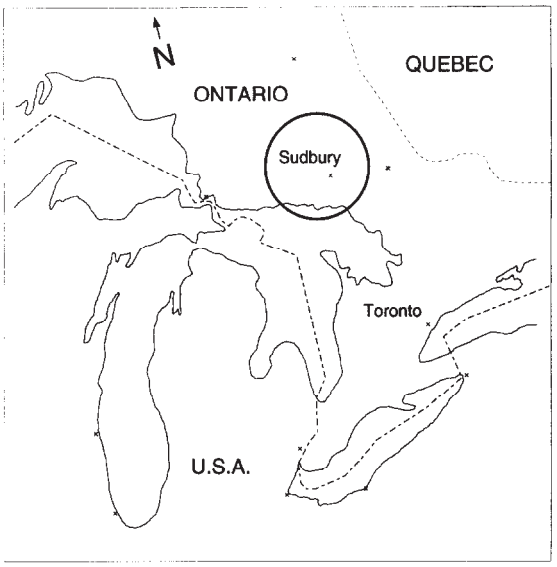

Fig. 1. Location map of Sudbury, Northern Ontario. The Copper Cliff tailings are located just outside Sudbury.

The impoundments form a relatively flat body which covers the bedrock to a depth of 20–30 m as shown in the cross-section of Fig. 3. The water table follows the topography and is about 2–5 m below the surface. The elevated tailings are, therefore, a local groundwater recharge zone. Modeled flow studies (Coggans, 1992) suggest that the water moves downward and then laterally outward along the tailings–bedrock boundary.

Tailings solids are fine-grain to silty sands containing 1–7 wt% sulfide minerals, mainly as pyrrhotite. The grain size and the porosity (~ 0.5) are relatively homo-

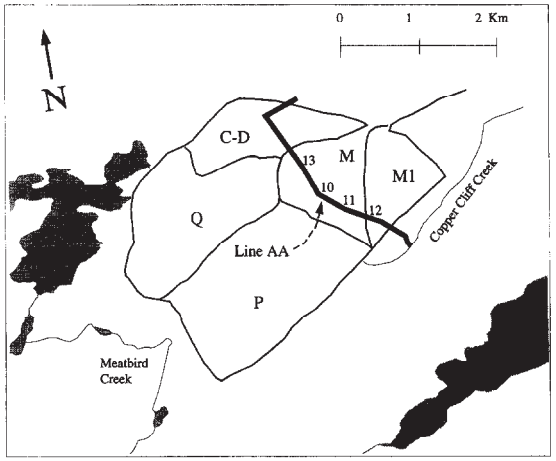

Fig. 2. The Copper Cliff tailings disposal site. The numbers along line *AA* indicate sampling wells IN13, IN10, IN11, and IN12.

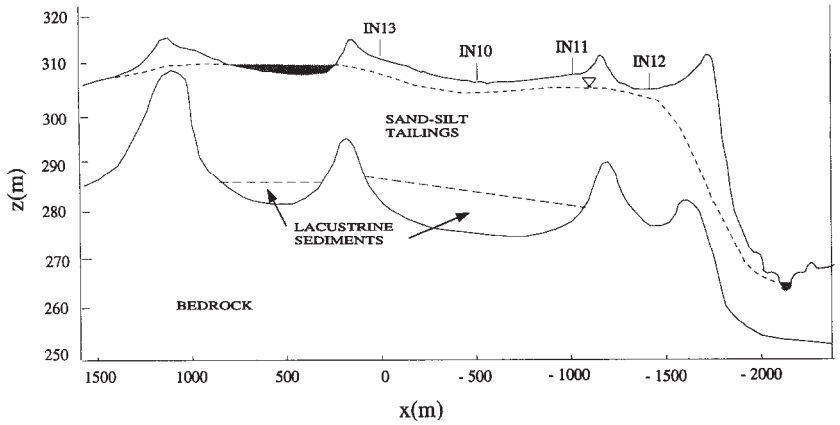

Fig. 3. Cross-section of line *AA*. The dashed line at the top indicates the approximate location of the water table. The vertical scale is exaggerated.

geneous throughout the area. Oxidation of sulfide minerals occurs within the unsaturated zone and results in low pH conditions and high levels of dissolved solids in the pore water. Contaminated groundwater from the tailings area recharges the local water system (Coggans, 1992) and, if not impeded and treated, may pose an environmental hazard.

The electrical conductivity of the dry and oxidized upper tailings layer (about 50 cm) is very low but, due to the acidic pore water, the conductivity below the water table is high-typically 70 mS/m. The conductivity of the bedrock beneath the tailings is low and does not exceed 0.5 mS/m. Some IP response is expected from the sulfides contained in the unoxidized tailings; negligible IP response is expected from the oxidized tailings or the bedrock.

3. Field survey and data

A time domain DC/IP survey was carried out along line *AA* shown in Fig. 2 which follows a major groundwater flow path in the tailings. Colinear dipole–dipole array data using $a = 10$ m and $n = 1$–6 were collected. Data acquisition problems were minimized because the impoundments are flat and relatively treeless. However, a few problems related to the special environment of the tailings were encountered. In particular, the high conductivity of the tailings required high input currents to get significant responses. Even with currents up to 10 A the measured voltages were low and prone to have low signal-to-noise ratio. The signal-to-noise ratio was even worse for the chargeability data which are generated from even lower voltages. Additionally, metal pipes, tanks, and fences scattered throughout the tailings area caused large interference responses in both the DC resistivity and IP data. The associated abnormal IP responses were characterized by large negative and positive apparent chargeabilities. Because their sources are metallic bodies much smaller than the scale of the modeling grid used for the forward and inverse calculations, they cannot be well represented mathematically and their calculated responses are frequently inaccurate. Fig. 4 shows a section of the time domain data in a line format. The irregularity and magnitude of variations of the data are obvious and typical of the entire line.

A pseudosection of the apparent conductivity is shown in Fig. 5. This pseudosection is broken into two parts for plotting purposes and also because there is a substantial difference in the magnitude of the data. High apparent conductivities are observed especially for data associated with small n-spacings. Low values appear from location -1500 to -1700 which indicate a deeper water table and, hence, a thicker dry and resistive tailings layer at the end of the line. Two anomalies manifested as a vertical set of closed contours, appear around locations -290 and -1160 and correspond to known metal pipe locations. The apparent chargeabilities, plotted in Fig. 6, are generally low. Higher values appear close to the northern end of the line around location 000 and between locations -1140 and -1500. Two anomalies coincide with the conductivity anomalies at -290 and -1160.

To assess three-dimensional effects, two additional surveys parallel to AA but located 30 m to the east and

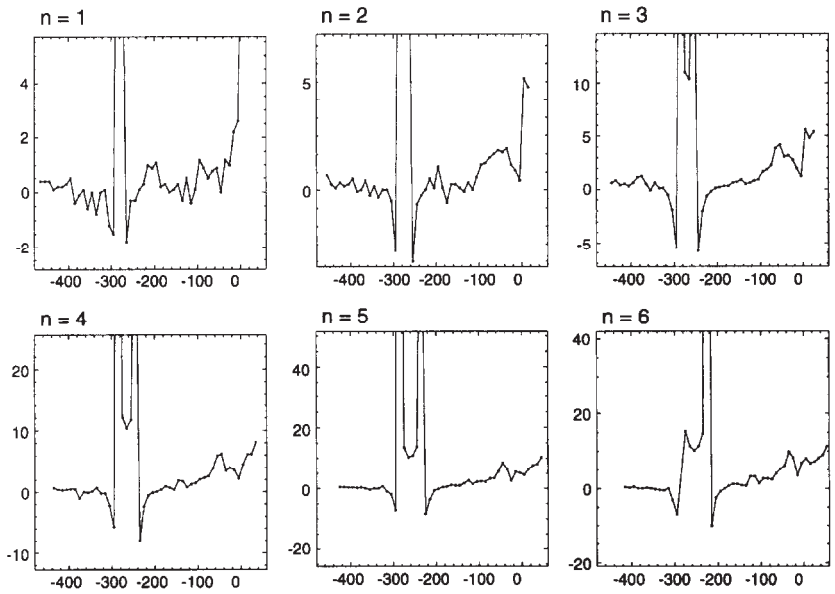

Fig. 4. Apparent chargeability data (mV/V) between locations 60 and −490 presented as separated line surveys, for $n = 1$–6. The large amplitudes associated with the pipe at −290 have been truncated for plotting purposes.

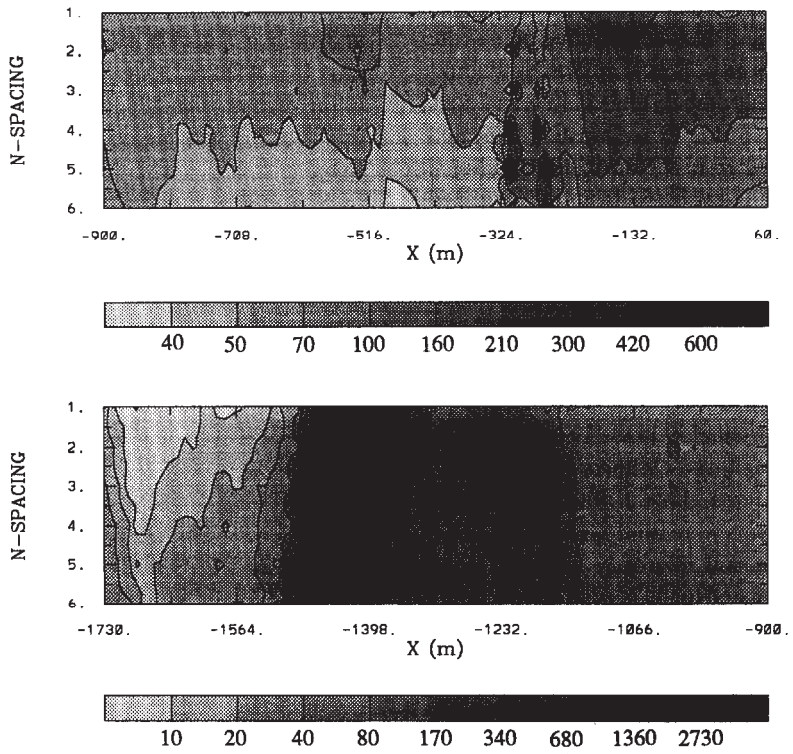

Fig. 5. The apparent conductivity pseudosection of line *AA* presented in two panels with different scales. The grey scales indicate conductivity in mS/m.

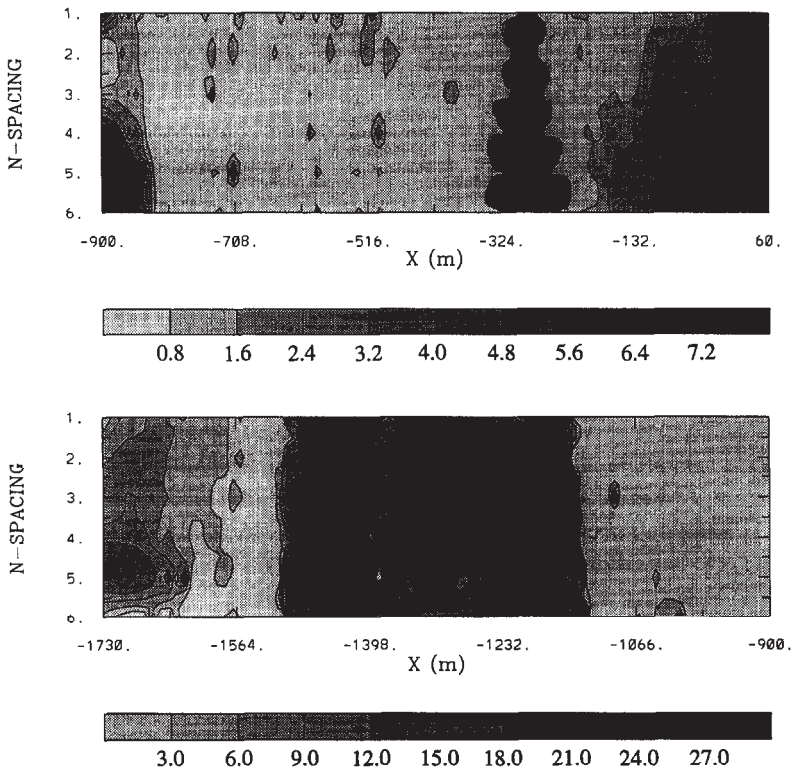

Fig. 6. The apparent chargeability pseudosection of line *AA* presented in two panels with different scales. The grey scales indicate chargeability in mV/V.

west were carried out. A phase domain system with dipole–dipole array, $a = 20$ m and $n = 1$–6 was used. Pseudosections derived for these parallel lines did not significantly differ from those in Figs. 5 and 6. This similarity provides some indication that 3-D effects may not be too important and that 2-D inversions might be applicable.

4. Inversion of the data

DC and IP data are inverted using computerized algorithms implementing the inversion methodology of Oldenburg and Li (1994). DC potentials are inverted directly to recover a 2-D conductivity structure. That conductivity is then used to generate the sensitivity matrix for the IP problem and the chargeability is obtained by solving a linear inverse problem. In the algorithm, the Earth is divided into many rectangular cells whose number greatly exceeds the number of data. In each cell, the conductivity and chargeability are assumed to be constant and the inverse problem is solved as an optimization problem where an objective function is minimized subject to the data constraints. A suitable model objective function which enables the inversion to find a model m with desired characteristics is:

$$\phi_m(m,m_0) = \beta_s \int\int w_s(m-m_0)^2 \mathrm{d}x\,\mathrm{d}z + \int\int \left\{ \beta_x w_x \left(\frac{\partial (m-m_0)}{\partial x} \right)^2 + \beta_z w_z \left(\frac{\partial (m-m_0)}{\partial z} \right)^2 \right\} \mathrm{d}x\mathrm{d}z \quad (1)$$

where m will be the logarithm of the conductivity for inversion of DC resistivity data, and it will be chargeability for inversion of IP data. The reference model is m_0 and the coefficients β_s, β_x and β_z weight the relative importance of the components of the objective function while w_s, w_x and w_z are functions which can be prescribed by the user. In discrete form, Eq. 1 can be written as:

$$\phi_m(\boldsymbol{m},\boldsymbol{m}_0) = \| W_m(\boldsymbol{m}-\boldsymbol{m}_0) \|^2 \quad (2)$$

where $\boldsymbol{m}$ and $\boldsymbol{m}_0$ are the parameterized model and the reference model, and W_m is a weighting matrix. The minimization of $\phi_m(\boldsymbol{m},\boldsymbol{m}_0)$ is carried out subject to the data constraints:

$$\phi_d(\boldsymbol{d},\boldsymbol{d}_0) = \sum_1^N \left(\frac{d_i^{\text{obs}} - d_i^{\text{pre}}}{\epsilon_i} \right)^2 = \phi^* \qquad (3)$$

where d_i^{obs} and d_i^{pre} are the observed and predicted data, respectively, ϵ_i is the assumed error in d_i^{obs}, and ϕ^* is a desired target misfit. Structural details of the recovered model are affected by ϵ_i and ϕ^* and, therefore, assigning values to these quantities is a matter of practical importance.

The assigned errors ϵ_i should include instrument inaccuracies, telluric noise, EM effects, errors arising due to 3-D effects, and discretization errors in the 2-D model. Estimating these errors is difficult and our final assigned error for each datum is composed of four terms. The first term is an error which is proportional to the absolute value of the datum. The second term is a constant value which is proportional to the mean value of the data. Variations in the data are manifestations of variations in the physical parameters; however, our confidence in a datum is weighted to decrease as its deviation from a reference average value increases. The third error term reflects this aspect. The reference average can be generated from the whole data set or it may pertain to the data from the relevant potential dipole. The last error term is intended to deal with outliers in the data which are related to the anomalous responses of small metal bodies. These cannot be represented properly by our parameterized model and, thus, such data are assigned large errors. Our final error assigning scheme is thus given by:

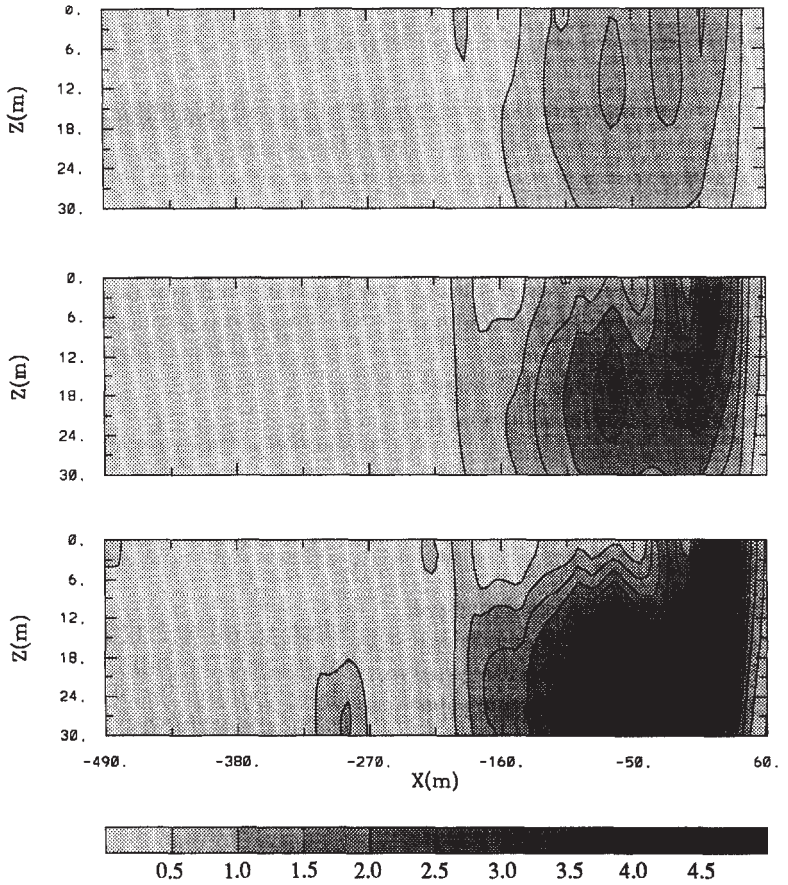

Fig. 7. Chargeability models of a section of line AA with misfits of (from top to bottom) $7N$, $6N$ and $5N$, where N is the number of data. The grey scale indicates chargeability in mV/V.

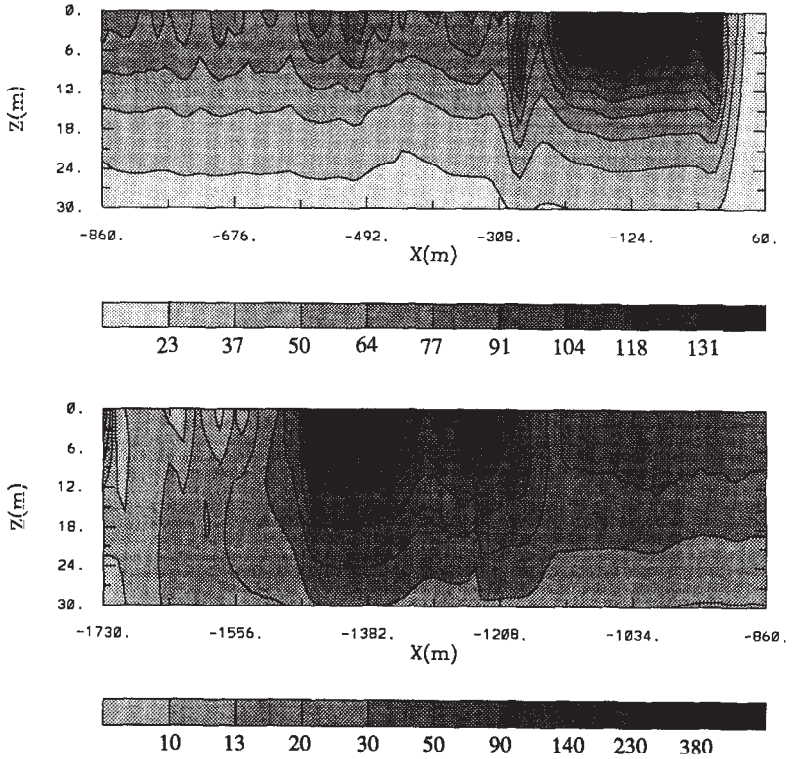

Fig. 8. The conductivity model of line *AA* presented in two panels with different scales. The grey scales indicate conductivity in mS/m.

$$ERR = A \cdot |DATUM| + B \cdot MEAN + C \cdot |DATUM - MEAN| + D \cdot E \quad (4)$$

where *ERR* is the assigned error of the *DATUM*, *MEAN* is the reference average value, and *A*, *B*, *C* and *D* are proportionality factors. The last term, *E*, is an exponential function of the ratio of the datum to the average value which increases rapidly when a datum value increases beyond a certain threshold. It is believed that the above method, although empirical and subjective, provides a reasonable relative weighting for the data errors.

The second decision focuses upon the value of the target misfit. Our experience is that this requires that a number of inversions be carried out at different misfit levels. Decreasing the misfit increases the model norm and tends to push features of the model to greater depth. We inverted each data set to a few levels of fit and chose the model which best fits our a priori understanding. As an example, we show in Fig. 7 three chargeability inversion results which fit the same data to levels of $7N$, $6N$ and $5N$ where N is the number of data and the misfit has been evaluated according to Eq. 3. The three models have common characteristics but the chargeability amplitudes and the depth of the main anomaly increase as the misfit decreases.

The final inversion results of the time domain data are given in Figs. 8 and 9. These models are in agreement with those obtained by inverting the phase domain data along the line and on the two adjacent parallel lines. The solution of the inverse problem is nonunique and we can generally produce many models which have the same global misfit to the data. Therefore, before we discuss these models we want to emphasize that some features of the models in Figs. 8 and 9 owe their existence to the chosen model objective function used in Eq. 1. For example, our objective function penalizes variations of the model in the vertical and horizontal directions, causing discontinuities to appear as smooth transitional features in our inversions. The structural details of the final model depend on the values of β_s, β_x, β_z, the value of the reference model m_0, and the functions w_s, w_x, and w_z in Eq. 1. Changing any one of these will produce a different model. To illustrate this point, we inverted a section of the DC data using a

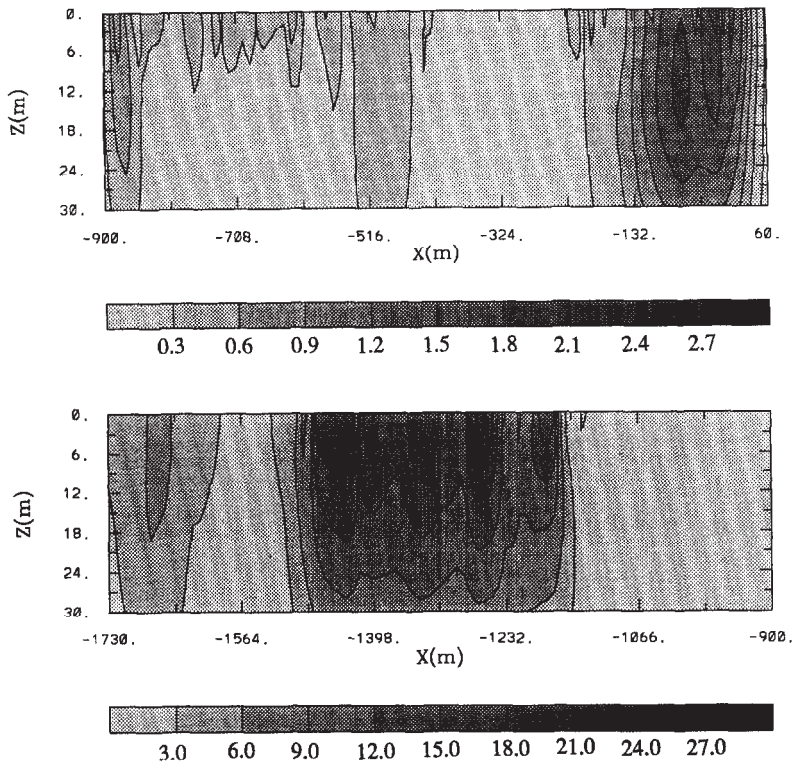

Fig. 9. The chargeability model of line *AA* presented in two panels with different scales. The grey scales indicate chargeability in mV/V.

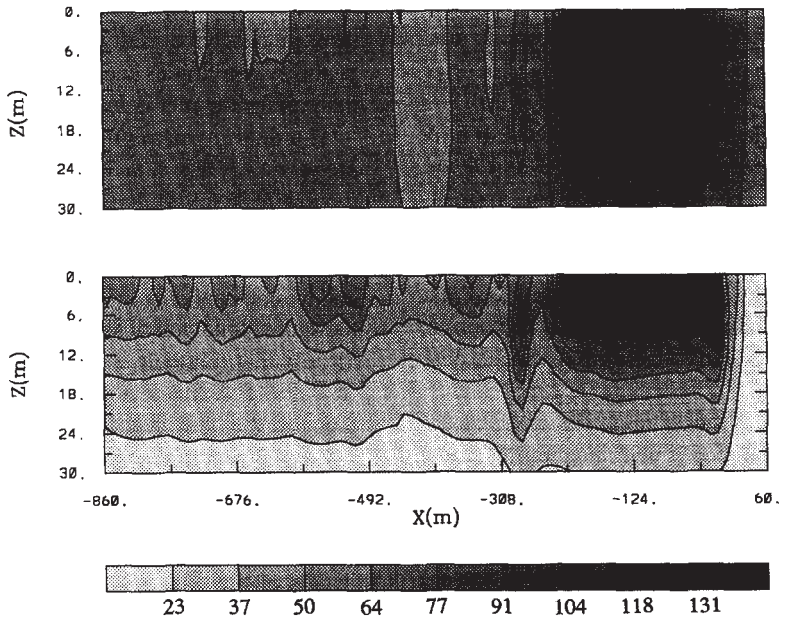

Fig. 10. The top panel is the conductivity model obtained by inverting data from the northern half of line *AA* but using a halfspace reference model of 70 mS/m. For comparison, the model recovered by inverting with a halfspace of 5 mS/m (the top panel in Fig. 8) is reproduced in the lower panel. Both models fit the data to the same level of accuracy. Differences between the two panels are due solely to the model objective function.

different reference model. For all the previous inversions we chose a 5 mS/m half space as the reference model. This is an intermediate value for expected conductivities of the tailings and the bedrock. As shown in Fig. 8, the conductivity decreases smoothly from the high conductivities close to the surface to the reference conductivity of 5 mS/m at depth. The fact that conductivities do not decrease below this value suggests that the surface experiment is not sensitive to the highly resistive bedrock. Inverting these same data but using a reference model of 70 mS/m, which is the typical conductivity in the tailings, yields the model of Fig. 10. For comparison, the model in Fig. 8 has been reproduced in Fig. 10. This shows that the surface conductivities from the two inversions are quite similar but there are significant differences with increasing depth. In fact, the depths at which the differences become substantial are related to the depth resolution of the DC resistivity method. Different models can also be generated by changing other parameters of the objective function. However, if some degree of smoothness in the horizontal and vertical directions is imposed then the models are quite similar to those in Figs. 8 and 9 in the top 10–15 m. We use those inversions to make our interpretations.

5. Interpretation and comparison with borehole data

Conductivity values along the line are typically about 70 mS/m. This is in agreement with data from the borehole located on the line and from penetrating cone data collected in its vicinity. Fig. 11 shows the agreement between the log data from borehole IN10 and the inverted conductivity at the borehole location (−510). Higher conductivities (up to 300 mS/m) can be found between locations 000 and −200 and locations −1140 and −1500. The dipping conductive layer from location −1500 to the end of the line likely reflects the dipping water table. The pipe at location −290 is imaged as a narrow vertical feature while the image of the pipe at location −1160 is masked by the surrounding higher conductivities.

The chargeability values are generally low. Higher values of about 1 mV/V appear between locations 000 and −150 and seem to concentrate at a depth of 12 m. The highest chargeabilities, ranging up to 20 mV/V,

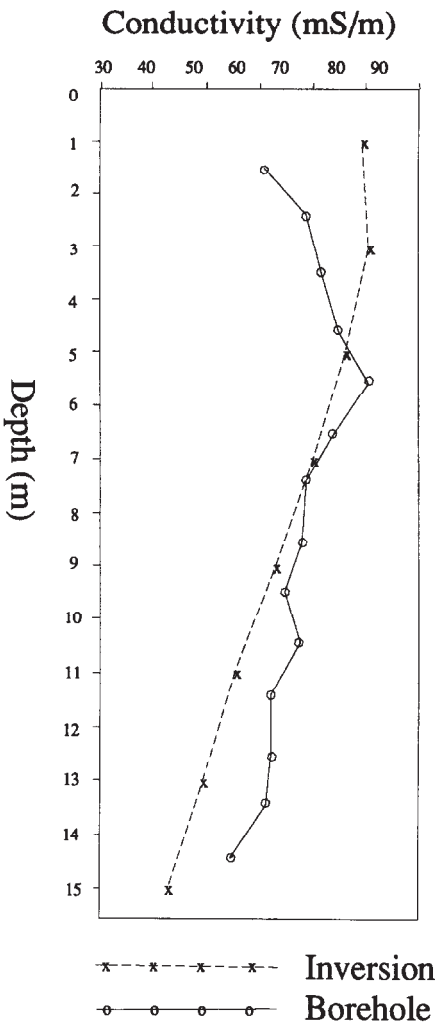

Fig. 11. The conductivity borehole log at IN10 and the corresponding conductivity obtained from the inversion.

appear between locations −1150 to −1500 and concentrate close to the surface.

There is a clear overlap of the main features in the conductivity and chargeability models. This is not unexpected since the source of conductivity, that is, the high level of dissolved solids in the pore water, is likely the product of the sulfide oxidation. Table 1 shows the conductivity and chargeability at locations of four sampling wells on the line with corresponding maximum TDS concentrations (Cherry et al., 1990) and estimated average sulfide concentrations (A. King, INCO Exploration and Technical Services Inc., pers. commun., 1994). The higher chargeabilities and higher known sulfide concentrations correspond to higher con-

Table 1
Sulfide concentration, maximum TDS concentration, average tailings conductivity, and chargeability at four sites

Site	Location	Average sulphides	[TDS] (mg/l)	σ (mS/m)	η (mV/V)
IN13	000	3%	10990	100	2
IN10	−510	<1%	3248	70	0.4
IN11	−1020	1.5%	2278	50	0.1
IN12	−1409	4%	10401	300	20

ductivities and higher known oxidation product concentrations.

6. Quantitative estimates of TDS and sulfide concentration

The goal of our research is to provide, using DC resistivity and IP surveys, the basic tools needed to quantitatively estimate the level of the existing contamination problem. That is, to provide a measure of the TDS concentrations and to predict the potential for further sulfide oxidation which is directly related to the sulfide concentrations.

6.1. Conductivity and TDS

Empirical and theoretical relations between dissolved ion concentrations and water conductivity exist (Merkel, 1972; Ellis, 1987; Worthington et al., 1990). Using Archie's law (Archie, 1942), the pore water conductivity can be related to the bulk conductivity of the formation. A direct relation between TDS concentration and rock conductivity can also be obtained (Ebraheem et al., 1990) from empirical results. As a control measure on our results and as an initial attempt to verify whether such relations can be used in acid mine drainage research in tailings, we applied relations given by Merkel (1972) and Ebraheem et al. (1990) to measurements taken in several sampling wells in the tailings.

Starting with the maximum ion concentrations given by Cherry et al. (1990) at four piezometers along the survey line, we calculated the tailings conductivities using two methods. The first was to obtain the pore water conductivity in the vicinity of the piezometers as a function of the sulfate concentrations using the empirical relation:

$$\log(\sigma_w) = 0.602 \log([SO_4]) + 0.2907 \quad (5)$$

derived from measurements given by Merkel (1972). In Eq. 5, σ_w is the pore water conductivity in mS/m and the sulfate concentration is in mg/l. Then, the tailings conductivity σ was computed using Archie's law:

$$\sigma = a\sigma_w\theta^m \quad (6)$$

where $\theta = 0.5$ is the porosity of the tailings and $a = 1.2$ and $m = 2.0$ are values typical of clay-free unconsolidated rock. The second method was to compute σ directly using the empirical formula given by Ebraheem et al. (1990):

$$\log(\sigma) = 0.6453 \log([TDS]) - 0.333 \quad (7)$$

These computed conductivities are compared in Table 2 with the conductivity obtained by the inversion. The comparison refers to the top 5 m where both ion concentrations and predicted conductivities achieve their maximum values. The conductivities computed by the first method are slightly lower since only sulfate concentrations were considered but both values agree, in general, with the conductivities obtained by the inversion at the corresponding sites. This is encouraging because it indicates that TDS concentration might reasonably be estimated from the inverted conductivities. However, the constants in Eq. 7 may still require evaluation for each tailings environment.

6.2. Chargeability and sulfide content

There are two primary difficulties to be overcome in order to obtain quantitative information about sulfide content from chargeability data. The first is to obtain estimates of the intrinsic chargeability by inverting the

Table 2
Maxima of major ion concentrations, calculated conductivities, and maximum inversion conductivity at four sites

Site	$[SO_4]$ (mg/l)	[Fe] (mg/l)	[Ni] (mg/l)	σ_M^a (mS/m)	σ_E^b (mS/m)	σ (mS/m)
IN13	8700	2190	–	138	188	100
IN10	3200	10	38	75	86	76
IN11	2200	77	1.5	60	68	72
N12	8700	1060	641	138	182	390

[a]Calculated using the relation from Merkel (1972).
[b]Calculated using the relation from Ebraheem et al. (1990).

IP data; the second is to establish a relationship between intrinsic chargeability and sulfide concentration. We have attacked the first problem in this paper, and although we feel that the relative values of chargeability in our inverted sections reflect true variations, the estimation of absolute values is made difficult because the degree to which the data should be fit is not known. The amplitude of the recovered chargeability increases as the data are fit to greater fidelity. Deciding what that misfit should be requires additional information. Borehole IP data acquired at a few places along the line would be particularly helpful in overcoming this difficulty. For the second problem, numerous studies of the relation between sulfide minerals concentration and chargeability have been carried out on natural samples and on artificial rocks (e.g. Collet, 1959; Anderson and Keller, 1964; Bacon, 1965; Scott and West, 1969). They all show a general trend of increasing chargeability with increasing sulfide content. Most investigators were concerned with the IP response of economical types of mineralization and only Anderson and Keller (1964) and Wardlaw and Wagner (1994) did work in a mine tailings environment. Thus, the exact correlation between the IP response and low sulfide concentration in tailings is unknown. Chemical analysis of tailings samples and borehole IP logs at the sampling site are needed to understand that relation.

7. Conclusions

The following conclusions are specific to the acid mine drainage research at the Copper Cliff tailings impoundments but could be relevant to other tailings areas and other mining waste disposal sites containing sulfide minerals.

Detailed conductivity structure of the tailings can be constructed by formally inverting the DC resistivity data. If the relationship between the conductivity and the TDS concentration can be established then the conductivity models can serve as a basis for quantitative mapping of the total dissolved solids. The relatively homogeneous porosity and grain size distribution throughout the tailings are a great advantage for accomplishing such a task. The fact that Ebraheem's formula, developed empirically from data at a different site, has worked well, is very encouraging.

Chargeability models, constructed by inverting IP data, can be used to locate areas of high sulfide concentrations. However, our results indicate that IP borehole logs are needed to calibrate the chargeability inversion results and an investigation of tailings samples is needed to tie the chargeability values to sulfide concentration. If such a relationship can be achieved, it will enable sulfide concentrations in the tailings to be mapped quantitatively.

Understanding the inversion methodology is crucial to achieving and properly interpreting the solutions of nonunique inverse problems. Inversion enables us to produce different models which fit the data to a specified degree. This is the basic advantage of the methodology but it might become a drawback if an inversion result, obtained by using inappropriately chosen parameters, is considered as the true and only candidate for interpretation. Our goal has been to construct a model which best represents the earth. This requires insight into the geological structure and expected variation of related physical parameters as well as some constraining in-situ measurements. This constructed model, together with the empirical relationships between conductivity and TDS and between chargeability and sulfide concentration, offers good potential for obtaining quantitative information about the environmental hazards posed by mine tailings.

References

Anderson, L.A. and Keller, G.V., 1964. A study in induced polarization. Geophysics, 29: 848–864.

Archie, G.E., 1942. The electrical resistivity log as an aid in determining some reservoir characteristics. Trans. Am. Inst. Miner. Metall. Eng., 146: 54–62.

Bacon, L.O., 1965. Induced polarization logging in the search for native copper. Geophysics, 30: 246–256.

Carpenter, P.J., Kaufman, R.S. and Price, B., 1990. Use of resistivity soundings to determine landfill structure. Ground Water, 28: 569–575.

Cherry, J.A., Robertson, W.D., Blowes, D.W. and Coggans, C.J., 1990. Hydrogeology and geochemistry of the INCO Ltd., Copper Cliff mine tailings impoundment. Waterloo Cent. Groundwater Res., Univ. Waterloo, Waterloo.

Coggans, C.J., 1992. Hydrology and geochemistry of the INCO Ltd., Copper Cliff, Ontario, mine tailings impoundments. Thesis. Univ. Waterloo, Waterloo.

Collet, L.S., 1959. Laboratory investigation of overvoltage. In: J. Wait (Editor), Overvoltage Research and Geophysical Applications. Pergamon, New York, NY, Ch. 5.

Draskovits, P., 1994. Application of induced polarization methods in integrated studies of ground water exploration and characterization of subsurface contamination. In: The John S. Sumner Mem. Int. Workshop Induced Polarization (IP) in Mining and The Environment. Dep. Min. Geol. Eng., Univ. Arizona, Tucson, AZ.

Ebraheem, M.W., Bayless, E.R. and Krothe, N.C., 1990. A study of acid mine drainage using earth resistivity measurements. Ground Water, 28: 361–368.

Ellis, D.W., 1987. Well Logging for Earth Scientists, Elsevier, Amsterdam.

Frangos, W. and Andrezal, T., 1994. IP measurements at contaminant and toxic waste sites in Slovakia. In: The John S. Sumner Mem. Int. Workshop Induced Polarization (IP) in Mining and The Environment. Dep. Min. Geol. Eng., Univ. Arizona, Tucson, AZ.

Kelly, W.E., 1976. Geoelectric sounding for delineating groundwater contamination. Ground Water, 14: 6–10.

Merkel, R.H., 1972. The use of resistivity techniques to delineate acid mine drainage in ground water. Ground Water, 10: 38–42.

Oldenburg, D.W. and Li, Y., 1994. Inversion of induced polarization data. Geophysics, 59: 1327–1341.

Scott, W.J. and West, G.F., 1969. Induced polarization of synthetic high resistivity rocks containing disseminated sulfides. Geophysics, 34: 87–100.

Stollar, R.L. and Roux, P., 1975. Earth resistivity surveys—a method for defining ground-water contamination. Ground Water, 13: 145–150.

Urish, D.W., 1983. The practical application of surface electrical resistivity to detection of ground-water pollution. Ground Water, 21: 144–152.

Wardlaw, S. and Wagner, R., 1994. Development of Waste Rock Sampling Protocol Using Induced Polarization. CANMET-MSL Div., Nat. Resour. Can., Ottawa, LR. 777-071, Final Rep.

Worthington, A.E., Hedges, J.H. and Pallat, N., 1990. SCA guidelines for sample preparation and porosity measurements of electrical resistivity samples. Log Anal., 31: 20–28.